The Effect of the Finite Ion Larmor Radius on the Kelvin-Helmholtz Instability

Melchior, H.; Popovic, M.

Publication date:
1967

Document Version
Publisher's PDF, also known as Version of record

July, 1967 Risö Report No. 158

The Effect of the Finite Ion Larmor Radius on the Kelvin-Helmholtz Instability

by

Henning Melchior and M. Popović

The Danish Atomic Energy Commission
Research Establishment Risö
Physics Department

Abstract

Excitation of the Kelvin-Helmholtz instability has been observed in a Q-machine when a sufficiently large velocity shear exists between adjacent layers of the plasma column.

In an interpretation of this observation, possible effects of the finite ion Larmor radius and the collisional viscosity were neglected. The purpose of our study is to remove the first of these simplifications. With the finite ion Larmor radius included, the growth rate of the instability is computed for several values of the velocity shear and different e-folding lengths of the density profiles.

Contents

1. Introduction

The purpose of this paper is to determine the effect of the finite ion Larmor radius on the Kelvin-Helmholtz instability in a fully ionized plasma. The possible occurrence of the Kelvin-Helmholtz instability in a fully ionized plasma immersed in a magnetic field has been treated by N. D'Angelo[1] and later by S. v. Goeler[2]. The effect of the finite Larmor radius was, however, not taken into account, and this paper describes an attempt to do so by the method indicated by K. V. Roberts and J. B. Taylor[3] and later used by F. F. Chen[4].

2. Assumptions about the Plasma

The ratio between the particle pressure and the magnetic pressure is supposed to be extremely small so that changes in the magnetic field due to the motion of the plasma can be neglected (low-β approximation). In a Cartesian frame of reference the magnetic field is taken to be oriented along the z-axis in the positive direction. A density gradient is supposed to exist along the x-axis, the unperturbed density distribution being of the form $n_0(x) = \bar{n}_0 e^{-\lambda x}$. The ions stream along the magnetic lines with a velocity that is constant along each line, but different for different lines. This shear in velocity may give rise to the Kelvin-Helmholtz instability.

3. Equations

The particle motion is described by the two-fluid equations, in which the effects of the finite Larmor radius is included via the viscosity stress tensor for the ions. The electron viscosity can be shown to be negligible.

The macroscopic equations for the ions are

$$\frac{\partial n_i}{\partial t} + \nabla \cdot (n_i \underline{v}_i) = 0 \qquad (1)$$

$$n_i m_i \left(\frac{\partial \underline{v}_i}{\partial t} + \underline{v}_i \cdot \nabla \underline{v}_i\right) = q n_i (\underline{v}_i \times \underline{B} - \nabla \varphi) - K T_i \nabla n_i - \nabla \Pi \quad . \qquad (2)$$

In addition we have an analogous set of equations for the electrons, in which, however, the viscosity term is neglected. In the collisionless limit the terms of the viscosity stress tensor are

$$-\Pi_{xx} = \Pi_{yy} = \frac{n_i K T_i}{\omega_{ci}} U_{xy}$$

$$\Pi_{zz} = 0$$

$$-\Pi_{xy} = -\Pi_{yx} = \frac{1}{2}\frac{n_i K T_i}{\omega_{ci}} (U_{yy} - U_{xx}) \qquad (3)$$

$$-\Pi_{xz} = -\Pi_{zx} = 2\frac{n_i K T_i}{\omega_{ci}} U_{yz}$$

$$-\Pi_{yz} = -\Pi_{zy} = 2\frac{n_i K T_i}{\omega_{ci}} U_{xz}$$

U_{ij} are the components of the divergenceless symmetrical velocity gradient tensor, often called the rate-of-shear tensor. The components are given by

$$U_{xx} = \frac{1}{3}\left(2\frac{\partial v_{iox}}{\partial x} - \frac{\partial v_{ioy}}{\partial y} - \frac{\partial v_{ioz}}{\partial z}\right)$$

$$U_{yy} = \frac{1}{3}\left(2\frac{\partial v_{ioy}}{\partial y} - \frac{\partial v_{iox}}{\partial x} - \frac{\partial v_{ioz}}{\partial z}\right)$$

$$U_{xy} = \frac{1}{2}\left(\frac{\partial v_{ioy}}{\partial x} + \frac{\partial v_{iox}}{\partial y}\right) \qquad (4)$$

$$U_{xz} = \frac{1}{2}\left(\frac{\partial v_{ioz}}{\partial x} + \frac{\partial v_{iox}}{\partial z}\right)$$

$$U_{yz} = \frac{1}{2}\left(\frac{\partial v_{ioz}}{\partial y} + \frac{\partial v_{ioy}}{\partial z}\right) .$$

When we consider a steady equilibrium solution of the type

$$v_{iox} = 0, \qquad v_{ioy} = \text{const.}, \qquad v_{ioz} = v_{ioz}(x)$$

with a constant or vanishing zero-order electric field in the x direction, the continuity equation and the y and z components of the momentum equation are automatically satisfied. The x-component of the momentum equation imposes the following conditions for the pressure gradient drift velocity v_{ioy}.

$$v_{ioy} = - \frac{c_i^2}{\omega_{c_i}} \lambda \; : \tag{5}$$

where

$$c_i^2 = \frac{KT_i}{m_i} \qquad \text{and} \qquad \omega_{c_i} = \frac{qB}{m_i} \; .$$

4. First-order Perturbed State

Stability conditions are obtained by analysing the perturbed, linearized macroscopic equations. In order to do so, we perturb the various quantities from the zero-order state by writing

$$n_i = n_{io} + n_{il} \; , \qquad v_i = v_{io} + v_{il} \; , \qquad \varphi = \varphi_o + \varphi_1 \; ,$$

where

$$n_{il} \ll n_{io} \; , \text{ etc.}$$

With these quantities in the governing macroscopic equations, and with higher-order terms neglected, one obtains after subtracting the zero-order equations:

$$\frac{\partial n_{il}}{\partial t} + n_{io} \nabla \cdot \underset{\sim}{v}_{il} + \underset{\sim}{v}_{il} \cdot \nabla n_{io} + \underset{\sim}{v}_{io} \cdot \nabla n_{il} = 0 \tag{6}$$

$$n_{io} m_i \frac{\partial \underset{\sim}{v}_{il}}{\partial t} + m_i n_{io} \underset{\sim}{v}_{il} \cdot \nabla \underset{\sim}{v}_{io} + m_i n_{io} \underset{\sim}{v}_{io} \cdot \nabla \underset{\sim}{v}_{il} + KT \nabla n_{il} +$$

$$qn_{io} \nabla \varphi_1 + qn_{il} \nabla \varphi_o - qn_{il} \underset{\sim}{v}_{io} \times \underset{\sim}{B} - qn_{io} \underset{\sim}{v}_{il} \times \underset{\sim}{B} + \nabla \cdot (\Pi_{io} + \Pi_{il}) - \nabla \cdot \Pi_{io} = 0. \tag{7}$$

We assume the solutions for small-amplitude perturbations to be of the form

$$\begin{aligned} n_{il} &= \bar{n}_{il} f(x) e^{i(k_y y + k_z z - \omega t)} \\ v_{il} &= V_{il}(x) \; e^{i(k_y y + k_z z - \omega t)} \\ \varphi_1 &= \varphi_1(x) \; e^{i(k_y y + k_z z - \omega t)} \; . \end{aligned} \tag{8}$$

With a zero-order density distribution

$$n_{io}(x) = \bar{n}_{io}\, e^{-\lambda x} \tag{9}$$

we have

$$\frac{\partial}{\partial x}\left(\frac{n_{il}}{n_{io}}\right) = \frac{1}{n_{io}}\frac{\partial n_1}{\partial x} + \lambda\frac{n_{il}}{n_{io}} \quad . \tag{10}$$

By assuming that the velocities are weak functions of x, and by making use of the equations (3), (4), (5), (8), (9), and (10), we can transform equations (6) and (7) to

$$-i\Omega\frac{n_{il}}{n_{io}} + ik_y V_{ily} + ik_z V_{ilz} - \lambda V_{ilx} = 0 ;$$

$$-i\Omega V_{ilx} - \omega_{ci} V_{ily} + c_i^2\frac{\partial}{\partial x}\frac{n_{il}}{n_{io}} + \frac{q}{m_i}\frac{\partial\varphi_1}{\partial x} =$$

$$\frac{c_i^2}{\omega_{ci}}\left[-\frac{i}{2}\lambda k_y V_{ilx} - \frac{1}{2}k_y^2 V_{ily} - k_y k_z V_{ilz} - k_z^2 V_{ily}\right] ;$$

(11)

$$-i\Omega V_{ily} + ik_y c_i^2\frac{n_{il}}{n_{io}} + ik_y\frac{q}{m_i}\varphi_1 + \omega_{ci} V_{ilx} = \frac{c_i^2}{\omega_{ci}}\left[-\frac{i}{2}\lambda k_y V_{ily} +\right.$$

$$\left.\frac{1}{2}k_y^2 V_{ilx} + k_z^2 V_{ilx} + ik_z\frac{n_{il}}{n_{io}}\frac{\partial v_{ioz}}{\partial x}\right] ;$$

$$-i\Omega V_{ilz} + \frac{\partial v_{ioz}}{\partial x} V_{ilx} + ik_z c_i^2\frac{n_{il}}{n_{io}} + ik_z\frac{q\varphi_1}{m_i} = \frac{c_i^2}{\omega_{ci}}\left[-i\lambda k_y V_{ilz}\right.$$

$$\left.-i\lambda k_z V_{ily} + k_y k_z V_{ilx} + ik_y\frac{n_{il}}{n_{io}}\frac{\partial v_{ioz}}{\partial x}\right] ;$$

where $\Omega = \omega - k_y v_{ioy} - k_z v_{ioz}$.

All terms on the right-hand side of the momentum equations come from the anisotropic pressure tensor and are due to the effect of the finite Larmor radius.

This system of four equations with five unknowns is completed by the z-component of the momentum equation for electrons. To obtain this equation, we will change q into -q, ω_{ci} into $-\omega_{ce}$, c_i^2 into c_e^2, and n_i into n_e in the corresponding ion equation. The terms which account for the finite Larmor radius effect are neglected. Since charge neutrality is preserved, this equation, in the limit $\frac{m_e}{m_i} \to 0$ and for equal temperatures $T_i = T_e$, is reduced to

$$c_i^2 \frac{\tilde{n}_{i1} f(x)}{\tilde{n}_{io} e^{-\lambda x}} = \frac{q \varphi_1}{m_i} \tag{12}$$

This gives the relation between perturbed density and potential. If the perturbation in the potential does not depend on x, the ratio n_1/n_o will be constant, i.e. $f(x) \equiv e^{-\lambda x}$.

The following dimensionless quantities were introduced for convenience:

$$\begin{aligned}
A &= \lambda \rho_i \quad (\rho_i = \frac{c_i}{\omega_{ci}}) \\
a &= k_y \rho_i \qquad b = k_z \rho_i \\
\phi &= \frac{\omega - k_y v_{ioy} - k_z v_{ioz}}{\omega_{ci}} \\
V^* &= \frac{V}{c_i} \\
k &= \frac{\lambda}{\lambda_\eta} = \frac{k_\eta}{k_\xi} = \frac{b}{a} \\
A &= \frac{1}{\omega_{ci}} \frac{\partial v_{ioz}}{\partial x}
\end{aligned} \tag{13}$$

Here ϕ is the frequency in the frame of the ions measured in units of ion cyclotron frequency while A is the non-dimensional shear in velocity.

Converting equations (11) into a non-dimensional form and eliminating the perturbation in the potential through (12), we obtain

$$
\begin{aligned}
&-\Delta V^*_{i1x} + ia V_{i1y} + ib V^*_{i1z} - i\phi \frac{\bar{n}_{i1}}{\bar{n}_{io}} = 0 \\
&(i\frac{a\Delta}{2} - i\phi_i) V^*_{i1x} + (\frac{a^2}{a} + b^2 - 1) V^*_{i1y} + ab V^*_{i1z} = 0 \\
&(1 - \frac{a^2}{2} - b^2) V^*_{i1x} + (i\frac{a\Delta}{2} - i\phi_i) V^*_{i1y} + (ibA + 2ia) \frac{\bar{n}_{i1}}{\bar{n}_{io}} = 0 \\
&(A - ab) V^*_{i1x} + ib\Delta V^*_{i1y} + (ia\Delta - i\phi_i) V^*_{i1z} + (2ib + iaA) \frac{\bar{n}_{i1}}{\bar{n}_{io}} = 0.
\end{aligned}
\tag{14}
$$

The condition that the determinant of this set of equations vanish gives the dispersion relation. By some algebraic transformations the determinant is brought into a form where the fourth-order algebraic equation becomes equivalent to an eigenvalue problem for the magnitude

$\varphi = (\omega - k_y v_{ioy} - k_z v_{ioz})/\omega_{ci}$

5. Computations and Results

The eigenvalue problem has been solved numerically on the IBM 7090 computer at the North European University Computing Center at Lyngby. In these computations the complex matrix was transformed to upper Hessenberg form by a modified version of the algorithm given by Dennis J. Mueller[5], connected with the QR-transformation procedure given by Axel Ruhe[6].

For each of the values of A (the non-dimensional shear in velocity), which was varied in 20 steps from 0 to 0.40, the dispersion relation was solved for 20 different values of k, the numerical value of the propagation vector. k was varied from an initial value of 10^{-4} to 1 in the following way:

$$k_n = k_{n-1} \exp(\frac{1}{5} \ln 10) \ .$$

This expression connects the actual value k_n with the value k_{n-1} used in the previous step. For a specific value of A, 20 different solutions of the dispersion relation are obtained (corresponding to the different values of k). Out of these solutions the one with the largest positive value of the imaginary part of the frequency is chosen since it will be the most unstable one.

In fig. 1 the values of the imaginary part of the frequency are plotted against A, the non-dimensional shear. In these calculations, $\lambda c_i/\omega_{ci} = 0.09$. Curves for different values of $a = k_y c_i/\omega_{ci}$ are shown.

It is seen that the growth rate of the instability increases as a is varied from 0.084 to a maximum of about 0.75. After this point, the growth rate decreases for a further increase in a. It may also be seen that in the case of large growth rates the onset of the instability occurs for small values of the shear A (see fig. 3).

The curves in fig. 2 show the imaginary part of the frequency for different values of Λ. It is seen that an increase in Λ has a stabilizing effect. In fig. 3 a comparison is presented between results of calculations performed with and without the finite Larmor radius terms. In general, these terms will have a stabilizing effect, but as curve II shows, there may be unstable solutions with the finite Larmor radius taken into account where calculations without it give no instability at all.

In fig. 4 the dependence of the real part of the frequency on the magnitude of the propagation vector is shown. It is seen that the frequency increases with increasing $k_y c_i/\omega_{ci}$, and that it is higher with the finite Larmor radius taken into account than without.

It is our intention later to verify experimentally the above results on the Q-machine at Risö. The results obtained in the present calculations support what has been found earlier by N. D'Angelo[1] and S. v. Goeler[2]. So it is not imperative to include the finite Larmor radius effect in the description of the Kelvin-Helmholtz instability experiment in a Q-machine. We feel, however, that through these calculations one obtains a more accurate description of the Kelvin-Helmholtz instability in a fully ionized plasma.

References

1) N. D'Angelo, Phys. Fluids 8, 1748 (1965).

2) S. v. Goeler, Phys. Fluids 9, 818 (1966).

3) K. V. Roberts and J. B. Taylor, Phys. Rev. Letters 8, 197 (1962).

4) Francis F. Chen, Phys. Fluids 8, 1323 (1965).

5) D. J. Mueller, Num. Math. 8, 72 (1966).

6) Axel Ruhe, BIT 6, 350 (1966).

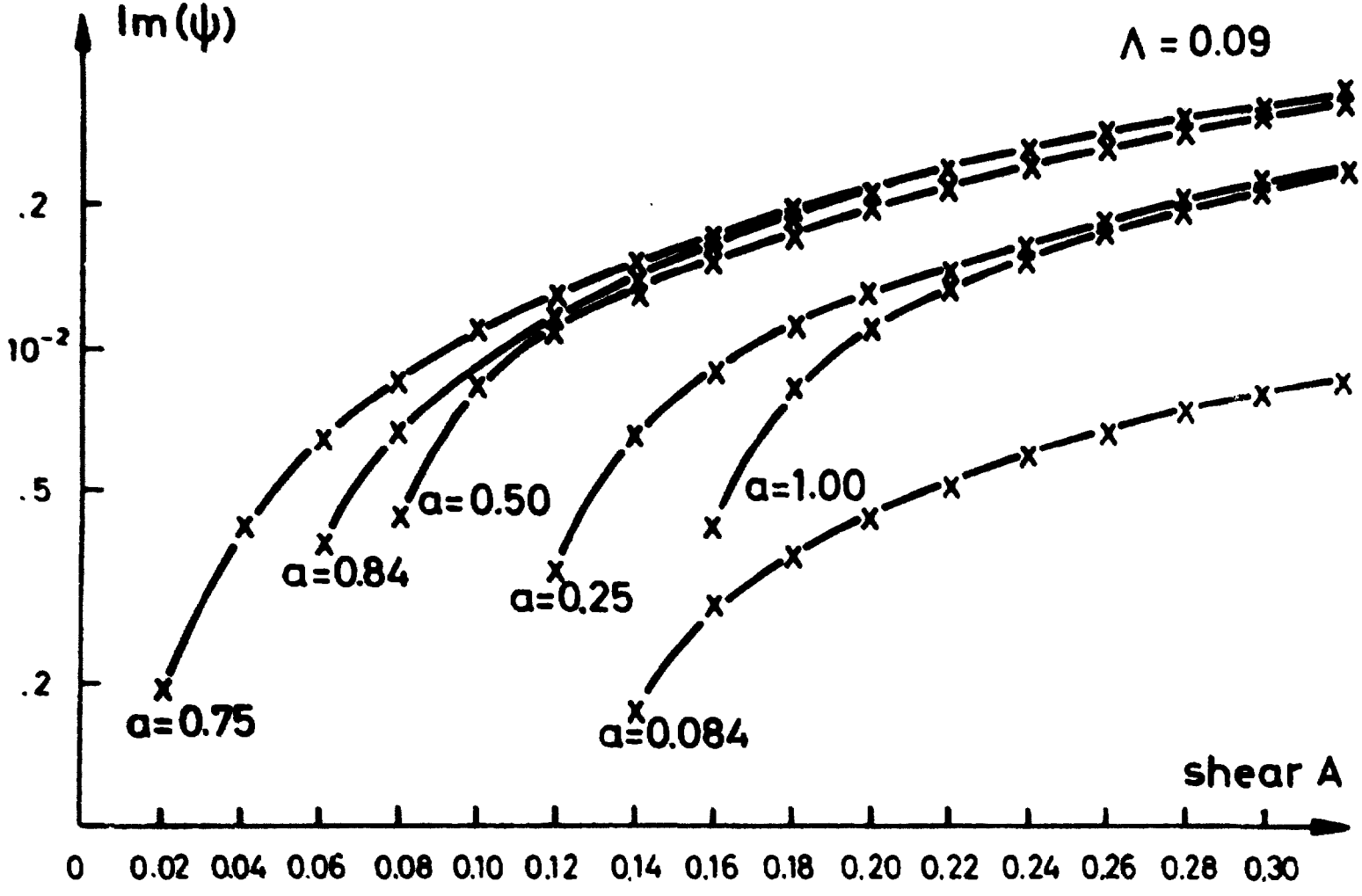

Fig. 1. Growth-rate for the instability as a function of the shear in velocity computed for different values of $a = k_y \rho_i$. For all curves $\Lambda = 0.09$

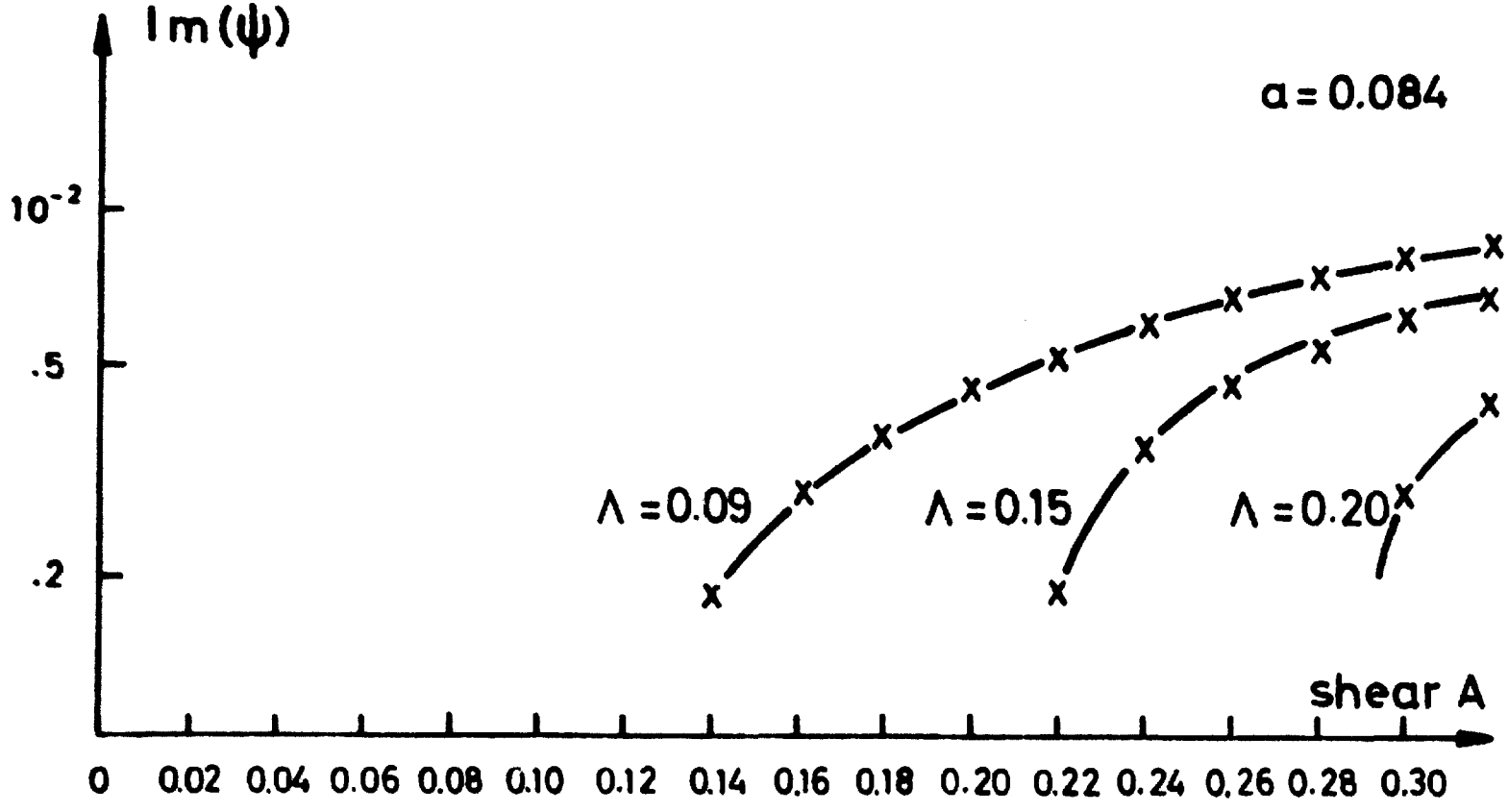

Fig. 2. Growth-rate for the instability as a function of the shear in velocity computed for different values of $\Lambda = \lambda\rho_i$. For all curves $a = 0.084$

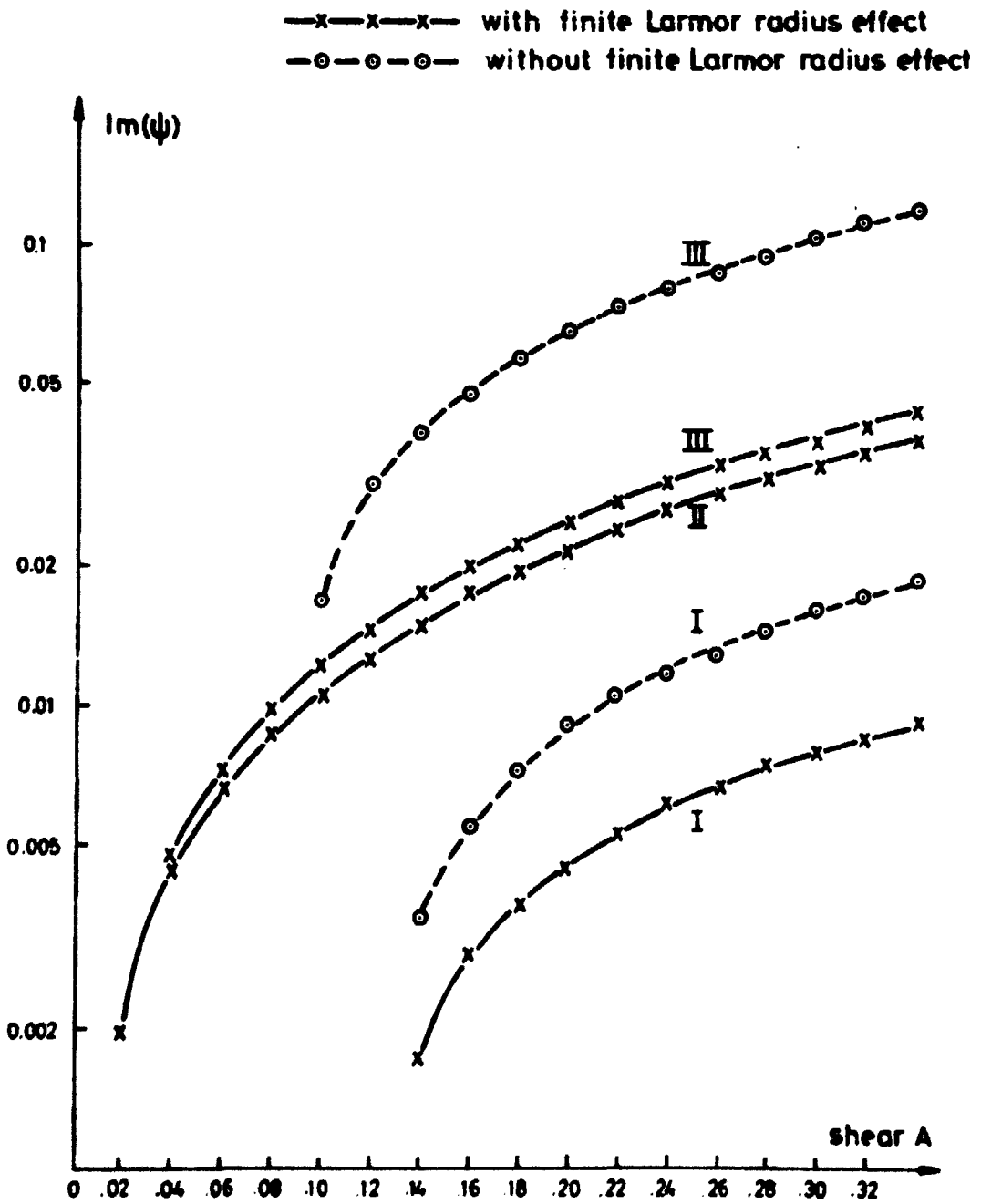

Fig. 3. The curves show the growth-rate of the instability for different values of $a = k_y \rho_i$ and $\Lambda = \lambda \rho_i$ computed with and without taking the finite Larmor radius effect into account. For the curves I $a = 0.084$ and $\Lambda = 0.09$. For curve II $a = 0.084$ and $\Lambda = 0.5$. For the curves III $a = 0.84$ and $\Lambda = 0.09$

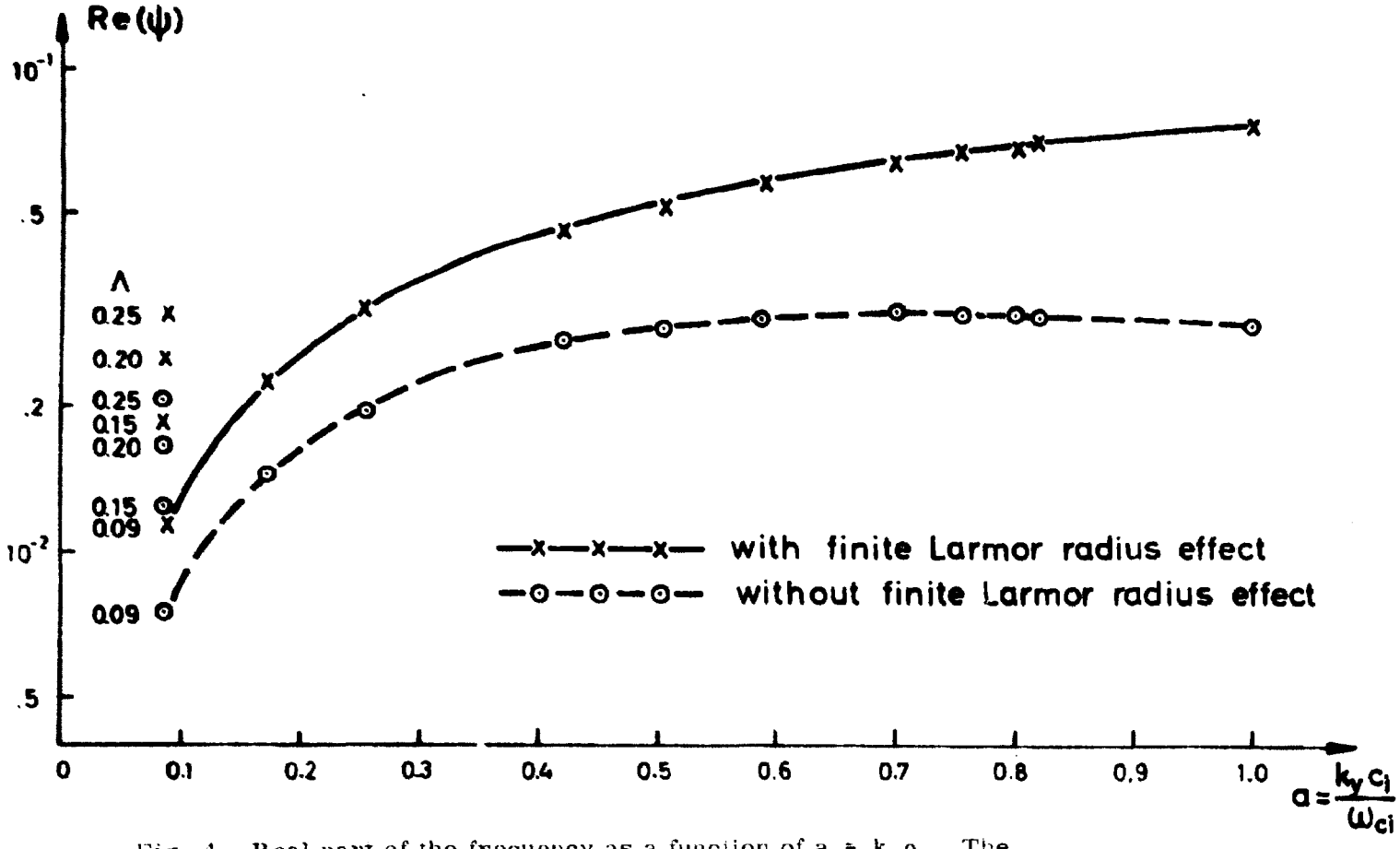

Fig. 4. Real part of the frequency as a function of $a = k_y \rho_i$. The curves for $\Lambda = 0.09$ are computed with and without finite Larmor radius effect.